Earthq Eng & Eng Vib (2018) 17: 771-785 **DOI**: https://doi.org/10.1007/s11803-018-0475-4

Direct use of peak ground motion parameters for the estimation of inelastic displacement ratio of SDOF systems subjected to repeated far fault ground motions

Cengizhan Durucan[1†] and Muhammed Gümüş[2‡]

1. *Department of Civil Engineering* (*Technology Faculty*), *Fırat University, Elazığ 23270, Turkey*

2. *Department of Civil Engineering, Gazi University, Ankara 06370, Turkey*

Abstract: This study is aimed at developing statistical equations to estimate the inelastic displacement ratio of single-degree-of-freedom systems subjected to far fault repeated earthquakes. In the study, peak ground motion parameters are used to define the scatter of the original data. The ratio of peak ground acceleration to peak ground velocity, and peak ground velocity of the ground motion records and structural parameters such as period of vibration and lateral strength ratio are used in the proposed equations. For the development of the equations, nonlinear time history analyses of single-degree-of-freedom systems are conducted. Then, the results are used in a multivariate regression procedure. The equations are verified by comparing the estimated results with the calculated results. The average error and coefficient of variation of the proposed equations are presented. The analyses results revealed that the direct use of peak ground motion parameters for the estimation of inelastic displacement ratio significantly reduced the scatter in the original data and yielded accurate results. From the comparative results it is also observed that results obtained using equations specific to peak ground velocity or peak ground acceleration to peak ground velocity ratio are similar.

Keywords: C1; peak ground velocity; peak ground acceleration; far fault ground motions; sequential ground motions

1 Introduction

In performance based design and analyses approaches, the displacement demand of a structure is calculated by using certain coefficients developed to transform the elastic displacement demand of single-degree-of-freedom (SDOF) systems to the inelastic displacement demand of a multi-degree-of-freedom (MDOF) system with structural degradation (Fajfar and Fischinger, 1988; Miranda, 1991; Miranda, 1999; Building Seismic Safety Council, 2000). The ratio of the maximum inelastic displacement demand of a non-degrading SDOF system to the spectral elastic displacement demand of the same SDOF system, C_1, (Building Seismic Safety Council, 2000; ATC, 2005; ASCE, 2007) is one of these coefficients. The stiffness or strength degradation properties of structures are considered by other coefficients such as C_2 (for stiffness degradation) and C_3 (for strength degradation) in FEMA356 (Building Seismic Safety Council, 2000), and C_2 (for stiffness degradation) and with a limit on R (for strength degradation) in FEMA440 (ATC, 2005).

Many studies were conducted for the development of statistical equations to estimate C_1 (Veletsos and Newmark, 1960; Miranda, 2001; Chopra and Chintanapakdee, 2004; Ruiz Garcia, 2011; Iervolino *et al*., 2012; Ruiz Garcia and Miranda, 2003 and 2006; Hatzigeorgiou and Beskos, 2009; Yaghmaei-Sabegh, 2012; Aydemir, 2013; Kabongo-Booto and Hatzigeorgiou, 2013; Durucan and Dicleli, 2015; Durucan and Durucan, 2016). In several studies, statistical equations are developed to estimate C_1 without separating the used ground motion data pool in terms of distance to nearest fault line. In contrast, in the recent studies (Ruiz Garcia, 2011; Iervolino *et al*., 2012; Kabongo-Booto and Hatzigeorgiou, 2013; Durucan and Dicleli, 2015; Durucan and Durucan, 2016) the ground motion data pools are classified according to their distance to closest fault line due to the special characteristics of near fault (NF) ground motion records distinguishing them from far fault (FF) ground motion records owing to their significant damage potential.

The majority of the studies, focused on the C_1, considered only the effects of the period, T, and strength ratio, R, of the considered SDOF systems and corresponding site class. Such generalized equations resulted in a large scatter in C_1 even if they were developed using data pools distinguished in relation to

Correspondence to: Cengizhan Durucan, Department of Civil Engineering (Technology Faculty), Fırat University, Elazığ 23270, Turkey
Tel: +98-3125823204
E-mail: cengizhandurucan@ahievran.edu.tr
[†]PhD; [‡]Msc

Received March 22, 2017; **Accepted** August 8, 2017

their closest distance to fault lines. However, design and analysis of structures is a complicated issue as it should consider both the: (i) structural and (ii) ground-motion uncertainties simultaneously. Accordingly, the attempts that do not consider soil, ground motion and structural parameters simultaneously may yield inaccurate results. Such design errors may lead to excessive costs or unexpected damage. In order to simultaneously account for the ground motion and soil effects together with the structural parameters, peak ground motion parameters may be used in the statistical equations developed to estimate the C_1 of SDOF systems.

Recently, in some studies (Akkar and Kucukdogan, 2008; Akkar and Özen, 2005) the effect of peak ground motion parameters on the variation of deformation demands of SDOF systems are considered to define the record to record variability. The main reason for the use of these peak ground motion parameters is the fact that they are dependent on ground motion and site properties. For example, A_p/V_p ratio (Durucan and Dicleli, 2015) and V_p (Akkar and Bommer, 2005) of a ground motion record includes information on the magnitude of the main earthquake, corresponding faulting mechanism, shear wave velocity of the soil, and distance of the recording site to the nearest fault line. Among these parameters, magnitude of the earthquake may be easily linked to the performance levels by the use of well known magnitude and return period relationships that are available for many regions of the world. The relationship between the earthquake magnitude and performance levels enable the use of developed equations and hence peak ground motion parameters in performance based analyses. Peak ground motion parameters also contain information about the frequency (Durucan and Dicleli, 2015) and energy content (Cosenza and Manfredi, 2000; Trombetti *et al*., 2008) of the ground motion. Moreover, Akkar and Özen (2005) illustrated the correlation of V_p with inelastic displacement demands of SDOF systems. Also, in the study of Cosenza and Manfredi (2000) it is stated V_p is representative of the damage potential of a ground motion as it is related with the energy content. In short, studies focused on the direct use of peak ground motion parameters for the estimation of inelastic displacement demands illustrated that peak ground motion parameters may correlate well with the inelastic seismic displacement demands of structures. Based on these findings, several studies (Durucan and Dicleli, 2015; Durucan and Durucan, 2016) developed equations to estimate C_1 by considering the A_p/V_p ratio of ground motion records. From these studies, it is observed that the scatter of the original data due to record to record variability, observed in calculated C_1 values, notably reduced.

Another important issue in the assessment of seismic induced risks is the probability of repeated earthquake loadings (Hatzigeorgiou and Beskos, 2009). Hatzigeorgiou and Beskos (2009) stated that repeated earthquake loadings may also create large deformation demands in comparison to single design earthquakes considered in structural codes. Repeated earthquake loadings may suffer seriously the structure that is already damaged and unrepaired by the first earthquake of the repeated loading array (Muria Villa and Toro Jaramillo, 1998). In contrast to the damage potential of the repeated earthquake loading, the number of studies focused on the effects of repeated earthquake loading is relatively low (Hatzigeorgiou and Beskos, 2009). In the studies focused on the response of systems subjected to repeated earthquake loading (Hatzigeorgiou and Beskos, 2009; Faisal *et al*., 2013; Hatzigeorgiou, 2010a and 2010b; Zhai *et al*., 2015), the peak ground motion parameters that may significantly reduce the record to record variability, are not considered. In this regard, in the study of Durucan and Durucan (2016), peak ground motion parameters on the variation of C_1 is used in combination with the effect of repeated earthquake loading for the structures subjected to NF ground motion records that contain significant velocity pulses.

In light of the above discussions, it is observed that a study considering the repeated earthquake loading conditions and peak ground motion parameters for the estimation of C_1 of structures subjected to FF ground motion records may provide valuable contributions to the subject area by reducing the record to record variability in the inelastic displacement demands of the SDOF systems and providing accurate estimations under the repeated earthquake conditions. Hence, in this study, new and easy to use A_p/V_p and V_p specific statistical equations are proposed for the estimation of C_1 of SDOF systems subjected to FF repeated earthquake loadings.

The proposed new A_p/V_p and V_p specific equations are aimed to complete a set of equations including two A_p/V_p specific equations proposed for SDOF structures subjected to FF and NF single earthquake loading (Durucan and Dicleli, 2015) and one A_p/V_p specific equation proposed for SDOF systems subjected to repeated NF earthquake loading (Durucan and Durucan, 2016). In the development of the proposed statistical equations, only ground motion records 20 km far from the fault line are considered. The equations developed in this study contribute to the subject area by the following beneficial properties: (i) the equations proposed in this study are developed and verified by using a large data pool only consisting of predefined FF ground motion records: (ii) the effects of A_p/V_p and V_p are considered to define the record to record variability of ground motion records and better estimate the calculated C_1 data, (iii) the effect of repeated earthquake loading (pre-shock, main shock, after shock) is considered to obtain the C_1 value, and (iv) the functional form of the proposed equations are kept as simple as possible. To the best of the authors' knowledge, the presented paper is the first study considering the effects of A_p/V_p or V_p in the estimation of C_1 of SDOF systems subjected to FF repeated earthquake loading.

The main parameters used in the study are: (i)

fundamental vibration period of the structure, T, (ii) lateral strength ratio, R,

$$R = \frac{mxS_a}{V_y} \quad (1)$$

where m is the mass of the structure, S_a is the spectral acceleration and V_y is the yield strength, (iii) A_p/V_p ratio or V_p of the design earthquake and (iv) repeated earthquake loading. The viscous damping ratio of systems with elasto-perfectly plastic hysteretic behavior is selected as 5%.The effect of parameters such as damping ratio, post-elastic stiffness, strength deterioration and stiffness degradation, and the systems subjected to NF ground motion records are not in the scope of this study.

The results and comparisons given in this study are based on the analyses of structures with periods smaller than 4 s. Structures with periods longer than 4 s are beyond the scope of this study. Also, note that the SDOF systems used in the analyses are not the full representatives of actual structures. In the performance based analyses, the results obtained using SDOF systems should be converted to the responses of actual structures, with higher mode effects and complex response and damage mechanisms, by applying appropriate and well defined procedures.

2 Parameters considered in the development of C_1

In the derivation procedure of the proposed equations, four main factors with a substantial effect on the variation of C_1 are considered. These parameters are: (i) the lateral strength ratio, R, (ii) the period of vibration of SDOF system, T, (iii) the A_p/V_p or V_p ratio of the design earthquake and (iv) presence of repeated earthquake loading.

Former research studies performed to investigate the variation of C_1 lead to a consensus approving the effect of R and T of the considered SDOF systems on the variation of C_1 (Miranda, 2001; Chopra and Chintanapakdee, 2004; Ruiz Garcia, 2011; Iervolino *et al*., 2012; Ruiz Garcia and Miranda, 2003 and 2006; Hatzigeorgiou and Beskos,2009; Yaghmaei-Sabegh, 2012; Aydemir, 2013; Kabongo-Booto and Hatzigeorgiou,2013; Durucan and Dicleli, 2015; Durucan and Durucan, 2016). Moreover, the effect of peak ground motion parameters (i.e., V_p and A_p/V_p) on the inelastic displacement demand of the structures is a relatively new topic. In this regard, the number of studies focused on the effect of these parameters is limited. Recent studies showed that peak ground motion parameters have notable effect on the inelastic displacement demands of structures (Akkar and Kucukdogan, 2008; Durucan and Dicleli, 2015; Liu and Zhang, 2016; Durucan and Durucan, 2016). A_p/V_p and V_p are specific parameters that represent several characteristics of the design earthquake (i.e, energy and frequency content). Moreover, the A_p/V_p ratio (Durucan and Dicleli, 2015) and V_p (Akkar and Bommer, 2005) are given as a function of combined effects of earthquake magnitude, faulting mechanism, distance to fault and soil conditions. Design earthquakes with small A_p/V_p ratios (i.e., $A_p/V_p < 5$) have a higher damage potential than those with high A_p/V_p ratios (i.e., $A_p/V_p > 20$) (Durucan and Dicleli, 2016) when they have identical A_p values. The effect of repeated earthquake loading is also considered in this study due to the information presented in the recent studies (Hatzigeorgiou and Beskos, 2009; Hatzigeorgiou, 2010a and 2010b), which illustrated the possible amplification of inelastic displacement demands calculated using single earthquake loading scenarios.

In many studies, the variation of C_1 with R, T, A_p/V_p and repeated ground motion loading is discussed and clearly highlighted. Since the effects of these parameters on the variation of C_1 have been studied by many researchers and have been clearly illustrated, the effect of these parameters on the variation of C_1 are not further investigated in this study. However, in the following section, the effect of V_p on the variation of C_1 is illustrated with parametric analyses and figures.

3 Effect of V_p on the variation of C_1

In the study of Akkar and Özen (2005), it was stated that the correlation of V_p of a ground motion record with inelastic displacement demands of SDOF systems are notable and may be even stronger than that of the A_p/V_p ratio of a ground motion record. Based on this stated observation and the findings of Akkar and Bommer (2007) showing the relation of V_p with earthquake magnitude, site class, distance to fault and type of faulting mechanism, the effects of V_p on the variation of C_1 is also investigated in this study.

In Fig. 1, scatter of C_1 data is plotted for NEHRP site class D. As observed from the figure, the data is highly scattered in the full range of the period. It is also observed that the amplitude of the scatter is more notable in the short period range (i.e., $T < 1.5$ s).

Based on these observations, Figs. 2(a) and 2(b) are plotted to observe the distribution of C_1 data together with the equation proposed by ASCE-SEI 41-06 (2007)

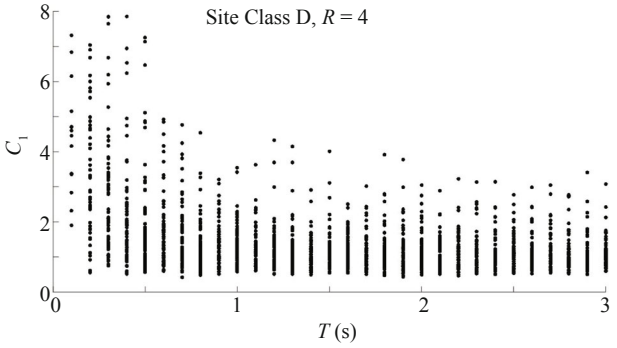

Fig. 1 Scatter of the C_1

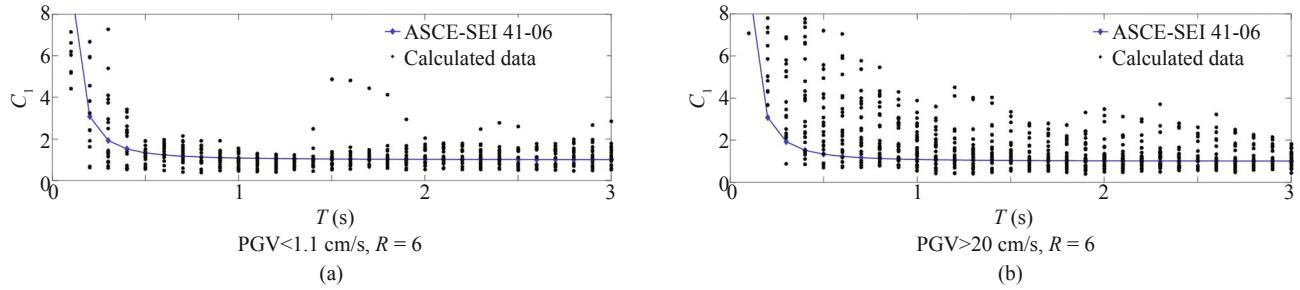

Fig. 2 Original C_1 data calculated using (a) weak and (b) strong ground motion records and the estimation of ASCE-SEI 41-06

for ground motion records with: (i) small PGV values (i.e., V_p < 1.1 cm/s) and (ii) higher V_p values (i.e., V_p > 20 cm/s), respectively. From Fig. 2(a), it is observed that the scatter of C_1 data is relatively low due to the fact that ground motions with small V_p values represent frequent earthquakes with limited damaging potential. In relation, it can be concluded that the equation proposed by ASCE-SEI 41-06 (2007) accurately estimates the original C_1 data for weak earthquakes. In Fig. 2(b), similar data is plotted for strong earthquakes with high damaging potential (i.e., ground motions with higher V_p values). In contrast to the observations from Fig. 2(a), Fig. 2(b) shows the significant scatter of C_1 data due to amplified record to record variability. It is also observed that the equation proposed by ASCE-SEI 41-06 (2007) generally underestimates the calculated C_1 data especially in the short period range (i.e., T < 1.5 s).

In Fig. 3, calculated C_1 data (obtained from ground motion records with variable site classes, variable distance to faults and variable earthquake magnitudes) are grouped in relation to their V_p ranges and plotted as a function of T for R = 6. From Fig. 3, it is observed that C_1 values gradually decrease for decreasing V_p values for the short period range (i.e., T < 1.5 s). The plots in Fig. 3 follow a clear trend as a function of the V_p range. The bandwidth formed by the scatter of data (Fig. 1) is simulated by the flare of the plots given for varying V_p values. In short, the figures presented in this section highlighted that the direct use of V_p in the calculation of C_1 is a meaningful method to reduce the record to record variability of ground motion data. The parameters required to estimate the V_p of the design ground motions are generally readily available from a site specific report or a ground motion prediction equation. Therefore, in this study, the V_p is also used for the formulation of C_1

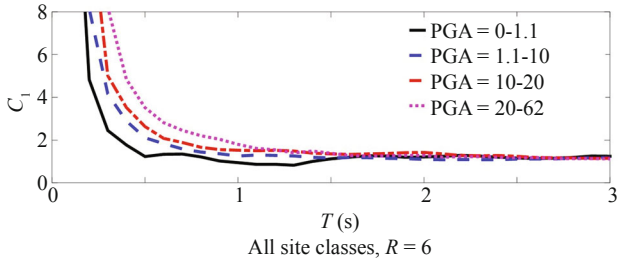

Fig. 3 Variation of mean C_1 data as a function of V_p

to consider the coupled effects of design ground motion (i.e., magnitude and faulting mechanism) and local site parameters (i.e., distance to fault and site class).

4 Repeated earthquake loading

It is known that earthquakes are typically followed by aftershocks (Changhai *et al*., 2018). If the magnitude of the aftershock is greater than that of the main shock, the main shock is called a foreshock (Shcherbakov *et al*., 2005). Therefore, structures may be exposed to seismic loading sequences (foreshock, main shock, aftershock) instead of one single earthquake loading. Recently, the number of studies focused on the response of structures subjected to repeated earthquake loading increased. In this regard, the statistical equations proposed in this study are dedicated to illustrate the effect of repeated earthquake loading on the inelastic displacement ratio, C_1. However, simulation of earthquake loading sequences is very hard due to variable characteristics of repeated earthquake loadings (Hatzigeorgiou and Beskos, 2009). Although earthquake loading sequences are variable, they can be defined with several scaling laws (Shcherbakov *et al*., 2005): (i) Gutenberg- Richter magnitude - frequency scaling law, (ii) Bath's law and (iii) the modified Omori's law. Details and implications of these laws may be found in Scherbakov (2005). In this study, as a practical approach (Faisal *et al*., 2013), artificial repeated earthquake loading scenarios generated by the scaling of real events are used. The details of the employed procedure are given in Hatzigeorgiou and Beskos (2009). Note that in Hatzigeorgiou and Beskos (2009), several alternative sequential loading simulations are presented. These alternatives are the repetition of the same earthquake two or three times or repetition of the same earthquake loading by scaling its original A_p with a factor. According to the authors, the last alternative presented in Hatzigeorgiou and Beskos (2009) is more realistic than the others. In this simulation method, the main shock is followed and preceded by two earthquakes with smaller peak ground accelerations. In this regard, the last approach presented in Hatzigeorgiou and Beskos (2009) is used in the study. The derivation of repeated earthquake loading scenario is based on: (i) Gutenberg – Richter (1944), and (ii) Joyner and Boore

relationships (1982) (i.e. relationship between the magnitude of an earthquake and the related peak ground acceleration value). In the employed procedure, the artificial foreshocks and aftershocks are calculated by scaling down the acceleration values of the main record with a ratio (i.e., 0.8526) governed by the relationship between the magnitude of successive earthquakes that occurred in the same region (Hatzigeorgiou and Beskos, 2009; Faisal *et al*., 2013; Hatzigeorgiou, 2010a and 2010b). In Hatzigeorgiou and Beskos (2009), it is stated that this ratio is irrespective from the magnitude and site to source distance.

By using the employed scaling procedure, one main and two smaller earthquake loadings (i.e, foreshock and aftershock) are combined by adding the acceleration – time relationship of the main and generated shocks. Other details on the simulation of repeated earthquake loading can be found in the literature (Hatzigeorgiou and Beskos, 2009; Faisal *et al*., 2013; Hatzigeorgiou, 2010a and 2010b). An example of accelerograms formed by the combination of one main and two smaller shocks is presented in Fig. 4.

5 Research methodology

The development procedure of the proposed statistical equations is presented in this section. In the development procedure, an in-house code is used to calculate the maximum elastic and inelastic displacement demands of SDOF systems subjected to selected ground motion data as a function of T and R. Next, the functional form of the proposed statistical equations is selected in relation to the previously presented functional forms in similar studies. Then a multivariate nonlinear regression procedure is performed to obtain the numerical values of constants used in the functional form of the proposed equations. In the regression analyses, the practical aspects of the relationship between T and R are also taken into account. This is achieved by eliminating the data that are unlikely to occur in practical conditions. This elimination is based on the study of Erduran and Kunnath (2010) stating the unlikely condition of a structure with a high R value with a small T due to the correlation between the strength and stiffness of a structure. Table 1 lists the used lower-bound periods for varying R values.

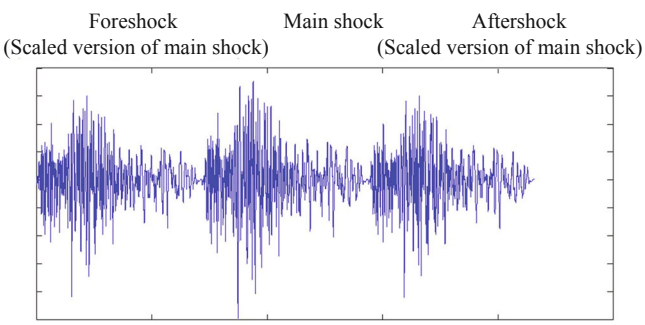

Fig. 4 Typical repeated earthquake loading obtained by adding the accelerograms of two scaled and one original ground motion record

Then, the accuracy of the proposed equations are visually tested by comparatively plotting the results (C_1 vs. T plots as a function of R) from the proposed equations together with their exact counterparts calculated by using the nonlinear time history analyses. Note that the ground motion data used in the verification of the proposed equations are selected from a different ground motion data pool, which is not used for the development of the proposed equations. Next, the accuracy of the proposed equations are statistically tested to further verify the validity of the proposed equations. In the verification procedure, a commonly used error estimation method which is based on measuring the deviation of original data from the estimated data (as a function of T and R) is used. Full details about the error measurement procedure are presented in Section 9.

6 Ground motions used in the study

The acceleration vs. time relationships of the ground motion records used in this study are collected from the PEER strong motion database (2014). In the analyses, ground motion records with a site to fault distance greater than 20 km are used. The ground motion data is collected using the records of 40 major earthquakes that have occurred all over the world. The ground motion database used in the study consists of 306 FF ground motion records.

The verification of the proposed equations are performed by using the data from ground motion records which are not used in the development of the equations. On the other hand, the past experience from previous studies (Durucan and Dicleli, 2015) showed that A_p/V_p is an important factor but its values greater than 20 do not significantly affect the results. Based on this observations, the authors selected ground motion records with similar A_p/V_p ratios to cover an A_p/V_p range between 0 and 20 (i.e, average A_p/V_p = 3, 5, 7, 11, 13 and 21). These groups consist of seven ground motion records due to the fact that average data from seven ground motion records may be used as a single ground motion loading in the time history analyses of structures (FEMA, 2000). In short, six ground motion groups with seven individual ground motion data (6 × 7 = 42) are used in the verification of the proposed equations.

Table 1 Limit case for R and T values

R (lateral strength ratio)	Lower bound T (s)
2	0.30
4	0.40
6	0.60
8	0.60

Other ground motions (306-42 = 264) are used in the development of the proposed equations. A list of ground motion data used in the analyses are given in Table 2.

7 Development and verification of the proposed equations

In this section, the procedure used for the development of the proposed equations is presented. In the development of the equations T, R and A_p/V_p (or V_p) are used to define the variation of C_1. The functional form used for the proposed equations is chosen by using the procedure given in the study of Durucan and Dicleli (2015). In the procedure, the constraint that dictate that $R = 1$, $C_1 = 1$ is satisfied by: (i) adding a 1+ term to the equation and (ii) using R-1 term instead of R. Durucan and Dicleli (2015) illustrated that the power functions fit the variation of data in such statistical equations very well. In this regard, to simulate the effect of considered parameters, power function are used (i.e., $Y = aX^b$). Based on the stated aspects, the form of the proposed equation is chosen as follows:

$$C_{1s} = 1 + \frac{(R-1)^{s_2}}{s_1 T^{s_3}\left(\frac{A_p}{V_p}\right)^{s_4}} \tag{2}$$

In Eq. (2), s_1, s_2, s_3 and s_4, are constants to be determined by using the results of nonlinear multivariate regression analyses conducted by well known Gauss-Newton solution algorithm with Levenberg-Marquardt (Bates and Watts, 1988) modifications. The solution algorithm aims to minimize the deviations of the calculated data from their fitted counterparts.

For the development and verification of Eq. (2), 48960 (306 ground motion records × 40 periods × 4 strength ratios) new nonlinear time history analyses are performed on accelerograms obtained by adding one original and two scaled records. In the nonlinear multivariate regression analyses, four different R values (i.e., 2, 4, 6, 8) and 40 different T values (0.1 s < T < 4.0 s) are used. From the analyses, the regression constants are calculated as given in Table 3.

The final form of the proposed equation is given below

$$C_{1s} = 1 + \frac{(R-1)^{0.59}}{0.47T^{0.63}\left(\frac{A_p}{V_p}\right)^{0.59}} \tag{3}$$

The accuracy of the developed equation (Eq. (3)) is tested by comparing the estimated results with calculated C_1 values of ground motion records which are not used in the development of the proposed equation (Fig. 5). For this purpose, 42 additional ground motion records

Table 2 List of FF ground motion records

Earthquake name (Year)	Records	M	D (km) range	Earthquake name (Year)	Records	M	D (km) range
Borah Peak (1983)	1	5.1	25	Yountville (2000)	8	5.0	96-44
Friuli (1976)	1	5.9	41	Kozani (1995)	1	5.1	85
Irpinia (1980)-2	1	6.2	30	Lytle Creek	2	5.3	21
Anza (Horse Cany) (1980)	2	5.2	41	Livermore2 (1980)	2	5.4	28
Big Bear (1992)	2	6.5	45	Trinidad offshore (1983)	2	5.7	72
Borrego (1942)	2	6.5	58	Livermore (1980)	2	5.8	30
Central Calif (1954)	2	5.3	27	Taiwan SMART1 (1985)	2	5.8	45
Georgia (1991)	2	6.2	73-51	Norcia (1979)	2	5.9	36
Gilroy (2002)	2	4.9	61	Taiwan SMART1(5) (1981)	1	5.9	32
Imperial Valley (1979)	2	6.5	25	Whittier Narrows (1987)	9	6.0	72-23
Chi-Chi (1999)-05	3	6.2	152-88	N. Palm Springs (1986)	9	6.1	67-27
Friuli (1976)-01	3	6.5	102-33	Morgan Hill (1984)	8	6.2	54-27
Irpinia (1980)	3	6.9	53-21	Superstition Hills (1987)	2	6.5	26
Kern County (1952)	3	7.4	82-39	San Fernando (1971)	5	6.6	89-25
Borah Peak (1983)	4	6.9	83-88	Northridge (1994)	21	6.7	80-36
Cape Mendocino (1992)	4	7.0	40-29	Kobe (1995)	4	6.9	23-21
Duzce (1999)	5	7.1	188-26	Loma Prieta (1989)	26	6.9	83-40
Borrego Mtn (1968)	6	6.5	211-45	Landers (1992)	7	7.3	142-69
Chi-Chi (1999)-02	8	5.9	120-80	Tabas (1978)	3	7.4	195-151
Chi-Chi (1999)	89	7.6	162-24	Kocaeli (1999)	3	7.5	68-53

Table 3 Calculated regression coefficients for Equation 1

Equation 1	
s_1	0.47
s_2	0.59
s_3	0.63
s_4	0.59

are analyzed and grouped (i.e, six groups consisting of seven ground motions) in relation to their A_p/V_p ratios. Details of the ground motion records used in the verification procedure are given in Table 4.

When plotting the C_1-T relationships obtained by using Eq. (3), the average A_p/V_p values of the grouped ground motion records are used in the equation for each

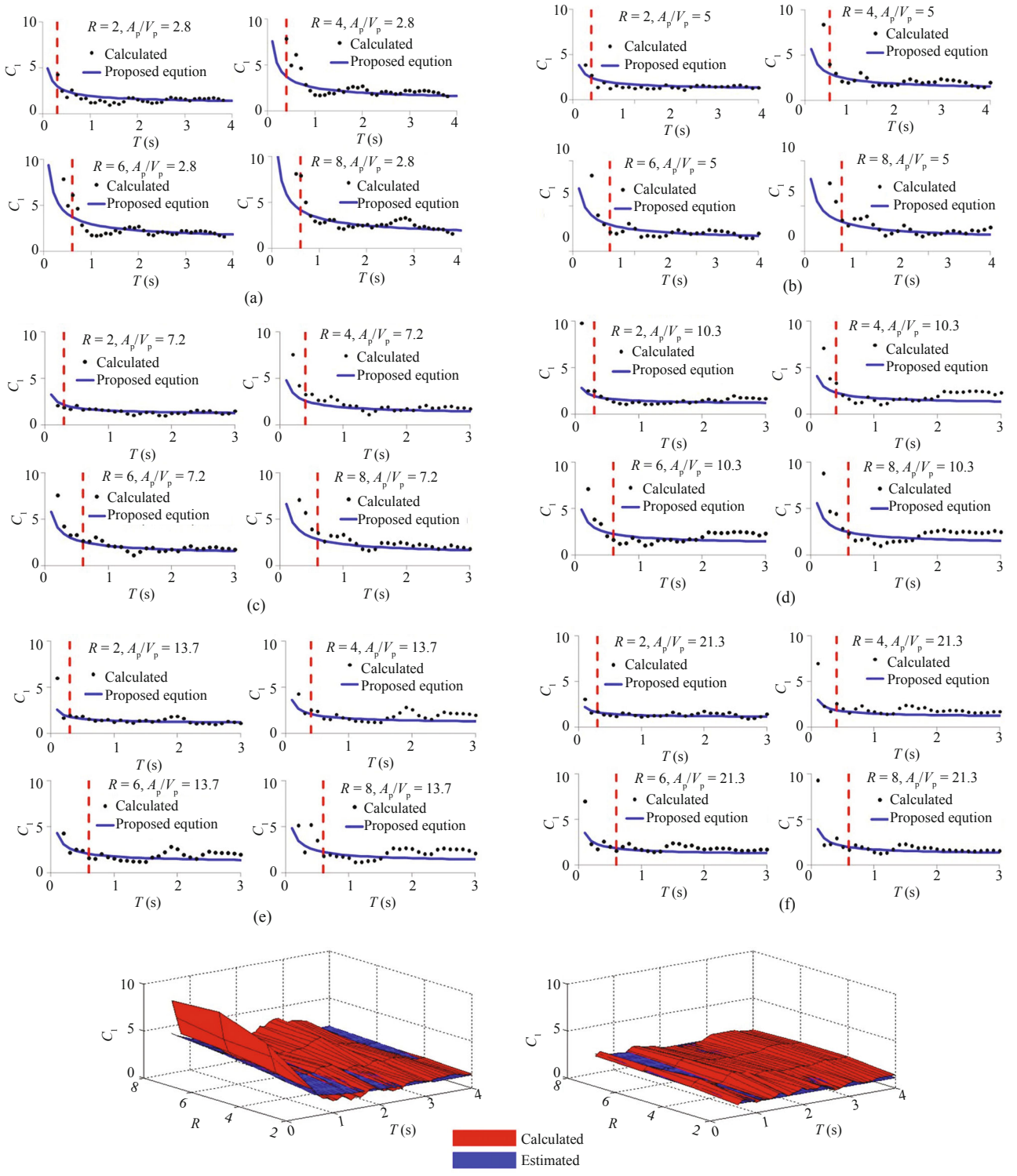

Fig. 5 Calculated values vs. estimated values of C_1 as a function of A_p/V_p a) A_p/V_p = 2.8, b) A_p/V_p = 5, c) A_p/V_p = 7.2, d) A_p/V_p = 10.3 e) A_p/V_p = 13.7, f) A_p/V_p = 21.3, g) A_p/V_p = 2.8 (3D plot), h) A_p/V_p = 21.3 (3D plot)

Table 4 Details of the ground motion records used in the verification of Eq. (2)

Station	A_p/V_p	Mean A_p/V_p	COV (%)	Station	A_p/V_p	Mean A_p/V_p	COV (%)
CHICHI/CHY026-N	2.0	2.8	24.0	KOBE/HIK000	8.9	10.3	9.0
KOCAELI/MNS090	2.1			KOCAELI/CNA000	9.5		
N.PALMSPR/SNY315	2.3			COALINGA/H-VYC110	10.0		
DUZCE/YPT060	2.7			COYOTELK/HVR240	10.2		
LANDERS/DWN090	3.4			KOBE/MZH090	10.9		
LANDERS/NHO270	3.4			CHALFANT/A-BEN360	11.1		
DUZCE/ARC270	3.5			HOLLISTR/B-HCH181	11.5		
KOCAELI/BLK180	3.6	5.0	18.4	KOCAELI/TKR090	12.3	13.7	9.3
CHICHI/CHY012-N	3.7			NORTHR/CAS000	12.7		
COALINGA/H-Z04000	5.2			CHICHI/TCU045-N	12.9		
AQABA/HAD-EW	5.5			Irpina-ITALY/B-MER000	13.3		
COALINGA/H-Z09090	5.5			NEWZEAL/B-MAT083	14.1		
KERN/PAS270	5.7			COALINGA/H-PG4090	15.1		
CHALFANT/A-TIN090	5.8			KOBE/MZH000	15.6		
LANDERS/BAD270	6.0	7.2	12.9	GEORGIA/ONI--Y	17.4	21.3	13.4
MORGAN/AGW240	6.3			N.PALMSPR/ARM270	19.6		
CHICHI/CHY074-N	6.6			LYTLECR/CLN090	20.2		
NCALIF/H-FRN314	7.3			NCALIF/D-SCA200	20.9		
LANDERS/JAB220	7.5			FRIULI/A-BCS000	21.9		
KERN/PAS180	7.9			CHALFANT/A-SHE009	22.8		
CHALFANT/A-LVL090	8.6			N.PALMSPR/H05360	26.4		

separate group. The comparative C_1-T relationships are plotted for four different R values (i.e, R = 2, 4, 6 and 8) and 30 different T values ranging between 0.1 and 3 s. The results in the longer period (i.e, $3 < T < 4$) range are not presented in the figures (except Figs. 5(a), 5(g), and 5(h)) due to negligible variation of results in this period range. In Fig. 5, the comparative results are presented for varying A_p/V_p and R values as a function of T. In the figures, the limit between the valid and invalid portion of the plots are defined with a vertical dashed line. In Figs. 5(g) and 5(h), the comparative results are presented in 3D to observe the variation of results with different parameters simultaneously. As stated before, the ground motion records (Table 4) used in the verification procedure are not used in the derivation of the proposed equation. From the figures, it is observed that the proposed equation generally produces results which are in good agreement with those calculated using nonlinear dynamic time history analyses. However, in Fig. 5(a) there is a more pronounced deviation between the estimated (Eq. (3)) and calculated results in the short period range for relatively high R values. This deviation is attributed to the relatively high record to record variability of very severe and very rare ground motions with very small A_p/V_p ratios (i.e. A_p/V_p = 2.8). The other plots showing the accuracy of the proposed equations revealed that the proposed equation, generally, accurately estimates the C_1 values calculated by using nonlinear time history analyses. In this regard, the proposed A_p/V_p specific equation may be used in the seismic analyses procedures of the structures subjected to FF repeated earthquake loadings.

The functional form used for the proposed V_p specific equation is chosen similar to the functional form of the proposed A_p/V_p specific equation (Eq. (3)). The nonlinear multivariate regression analyses performed by using the results of nonlinear time history analyses yielded the regression constants used in Eq. (4). The final form of the proposed V_p specific equation is obtained as given below;

$$C_{1s} = 1 + \frac{(R-1)^{0.55}}{2.11T^{0.55}(V_p)^{-0.17}} \tag{4}$$

Accuracy of the proposed V_p specific equation (Eq. (4)) is tested by the results of nonlinear dynamic analyses conducted by using the FF ground motion records representing repeated earthquake conditions. As in the previous case, the ground motion records used in the verification procedure are not used in the derivation of the proposed equation. The ground motion

records presented in Table 5 are modified to represent repeated earthquake loading and used in the verification procedure.

In Fig. 6, the analyses results are compared with the results obtained from the proposed equation (Eq. (4)). In the figures, the practical limits of the plots are defined with a vertical dashed line. In Figs. 6(g) and 6(h), the comparative results are presented in 3D to observe the variation of results with different parameters simultaneously. From Fig. 6 it is observed that the proposed equation generally produces results which are in reasonable agreement with those calculated using nonlinear dynamic time history analyses. The only exception of this conclusion is the plots given in Fig. 6(f) (i.e., Plots for V_p = 24 and R = 4, 6 and 8). From this figure, it is observed that there are deviations between the calculated and estimated results. In the ground motion group with average V_p ratio of 24 cm/s (Fig. 6(f)), the individual V_p values of the ground motions are 16, 17, 18, 24, 25, 33 and 39 cm/s. Although these ground motions are grouped together, the deviations in the V_p values of ground motions in the group are relatively high. In this regard, differences observed in the comparative results may be attributed to the use of an average V_p ratio with a relatively high coefficient of variation (i.e., %36) in the considered ground motion group. In general, the figures showing the performance of the proposed equations revealed that they were accurate. In this regard, the proposed equations may be used in the seismic design and analyses procedures of the structures.

8 Effect of repeated earthquake loading on C_1

The effect of repeated earthquake loading on the inelastic displacement ratios of SDOF systems is investigated in this section. For this purpose, the $C_1 - T$ relationships of SDOF systems are comparatively plotted using the equation proposed for single earthquake loading (Durucan and Dicleli, 2015) and Eq. (3) proposed for repeated earthquake loading (Fig. 7). The comparative results are plotted for the considered limit cases of strong (R = 2) and weak (R = 8) structural systems and varying mean A_p/V_p ratios of ground motions representing severe (A_p/V_p = 3) moderate (A_p/V_p = 10) and small (A_p/V_p = 20) earthquake loadings. From the figure, it is observed that the effect of repeated earthquake loading is not notable for strong structures (R = 2) subjected to moderate and small earthquakes. In contrast, the effect of repeated loading is higher for weaker structures (R = 8) regardless of the damage potential of the ground motion loading. Another observation from the figures is that the effect of repeated earthquake loading is generally higher for structures that fall in the short period range. The only exception of this observation is the case of severe earthquake loading. For the severe loading case (Figs. 7(a), 7(b)),

Table 5 Details of the ground motion records used in the verification of Eq. (3)

Record station/name	V_p	Mean V_p	C.O.V (%)	Record Station/Name	V_p	Mean V_p	C.O.V (%)
FRIULI/A-BCS000	1.3	2.2	30.6	HOLLISTR/B-HCH181	6.3	6.8	7.5
NCALIF/D-SCA200	1.5			COALINGA/H-PG4090	6.3		
LYTLECR/CLN090	1.6			CHALFANT/A-LVL090	6.4		
DUZCE/ARC270	2.5			NORTHR/CAS000	6.8		
GEORGIA/ONI--Y	2.6			CHALFANT/A-SHE009	7.0		
KOCAELI/MNS090	2.8			LANDERS/NHO270	7.4		
KOCAELI/TKR090	2.8			LANDERS/BAD270	7.5		
Irpina-ITALY/B-MER000	3.1	4.1	16.4	DUZCE/YPT060	7.9	11.3	24.7
AQABA/HAD-EW	3.4			COALINGA/H-Z09090	8.9		
NEWZEAL/B-MAT083	3.7			KERN/PAS270	9.2		
KOBE/MZH000	4.4			LANDERS/DWN090	11.3		
KOCAELI/BLK180	4.6			COALINGA/H-Z04000	12.6		
LANDERS/JAB220	4.7			COALINGA/H-VYC110	13.5		
KOBE/MZH090	4.7			KOBE/HIK000	15.6		
COYOTELK/HVR240	4.8	5.3	9.9	CHALFANT/A-BEN360	15.7	24.5	35.6
N.PALMSPR/H05360	4.9			CHICHI/CHY012-N	16.6		
MORGAN/AGW240	5.0			KOCAELI/CNA000	18.4		
N.PALMSPR/SNY315	5.1			CHICHI/CHY074-N	23.6		
N.PALMSPR/ARM270	5.2			NCALIF/H-FRN314	25.3		
KERN/PAS180	5.6			CHICHI/CHY026-N	32.6		
CHALFANT/A-TIN090	6.3			CHICHI/TCU045-N	39.0		

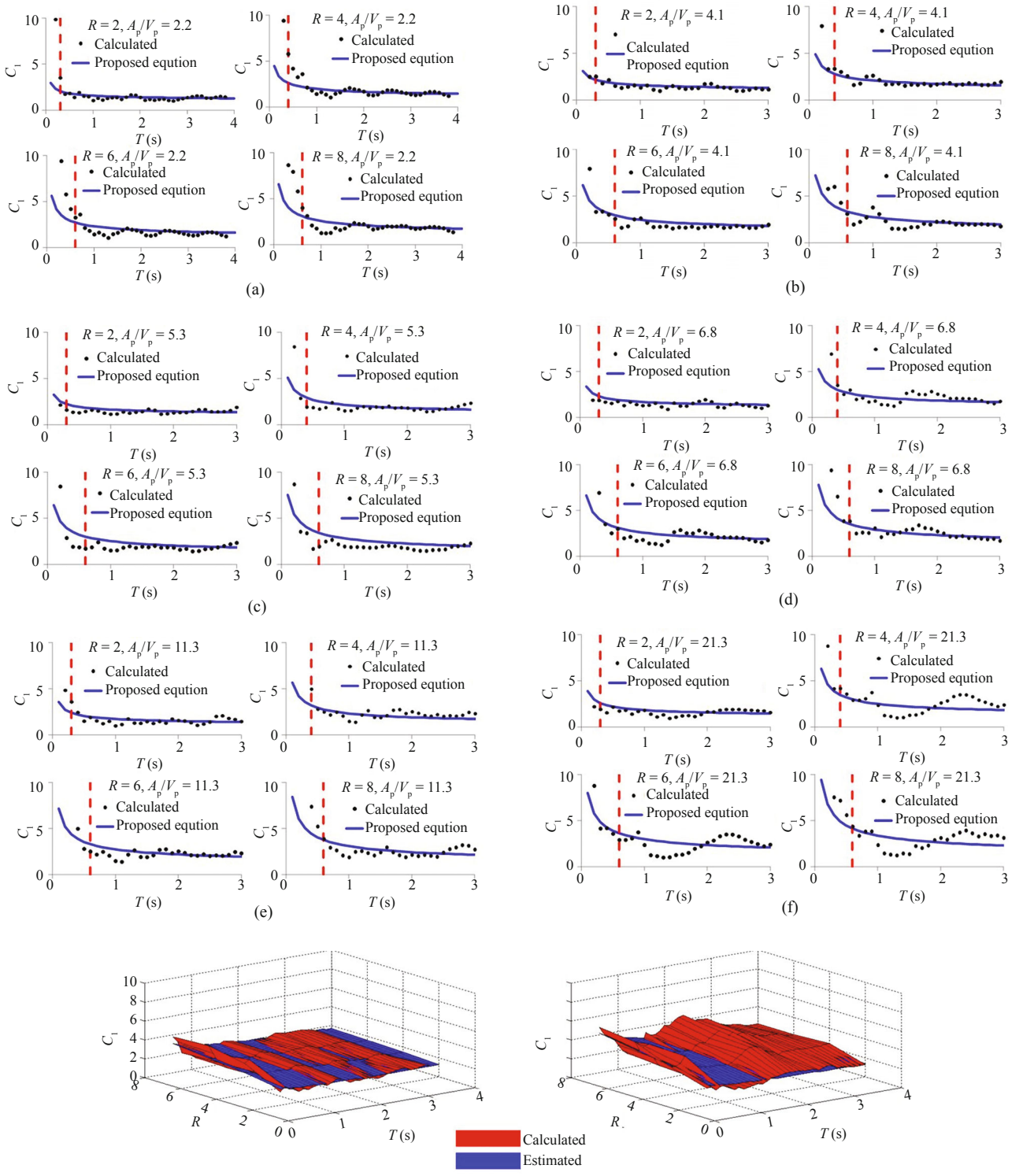

Fig. 6 Calculated values vs. estimated values of C_I as a function of V_p; a) V_p = 2.16, b) V_p = 4.09, c) V_p = 5.27, d) V_p = 6.81, e) V_p = 11.29, f) V_p = 24.46, g) V_p = 2.16 (3D plot), h) V_p = 24.46 (3D plot)

it is observed that the responses of strong and weak structures are similar for whole period range. The main reason behind this observation is the fact that the high amplitude acceleration region of a ground motion record with a small A_p/V_p ratio is relatively larger than those of ground motions with moderate and large A_p/V_p ratios. This leads to the pushing of structures to higher plastic displacement levels which results in the accumulation of displacements from consequent earthquakes.

9 Error measurements

In this section, the accuracy of the proposed statistical equations in estimating the calculated C_1 values are further evaluated using the error measurement criteria used in several studies (Ruiz Garcia, 2011; Durucan and Dicleli, 2015; Durucan and Durucan, 2016).

$$E_{TR} = \frac{1}{n}\sum_{i=1}^{n}\left[\frac{C_{1proposed\_i}}{C_{1calculated\_i}}\right] \quad (5)$$

where E_{TR} is the error measurement term, n is the number of used data, $C_{1proposed\_i}$ is the C_1 value estimated by the proposed equation and $C_{1calculated\_i}$ is the C_1 value calculated from nonlinear time history analyses of SDOF systems. The error measurements are employed for full T and R ranges of the data.

Results of the error measurements of Eqs. (3) and (4) are plotted together with associated coefficient of variation (COV) values in Figs. 8 and 9, respectively. In the calculation of the error measurement values, data obtained from 264 ground motion records employed in the derivation of the proposed equations are used. The coefficient of variation values given in Figs. 8(b) and 9(b) are calculated by taking the ratio of standard deviation of the data to the mean value as a percentage. In the figures, the line segments in the proximity of one shows that the proposed equations estimate the average values of actual results while the line segments above one represent a conservative estimation on the safe side.

In light of the above explanations, the results presented in Figs. 8 and 9 shows safe estimation trends for the whole T and R range, on average. In the figures, it is also clear that the proposed equations estimate the results closer to the mean of actual results for small R values (i.e., R = 2 and R = 4) representing strong and normal strength structures. On the other hand, for weaker structures with relatively high R values (i.e.,

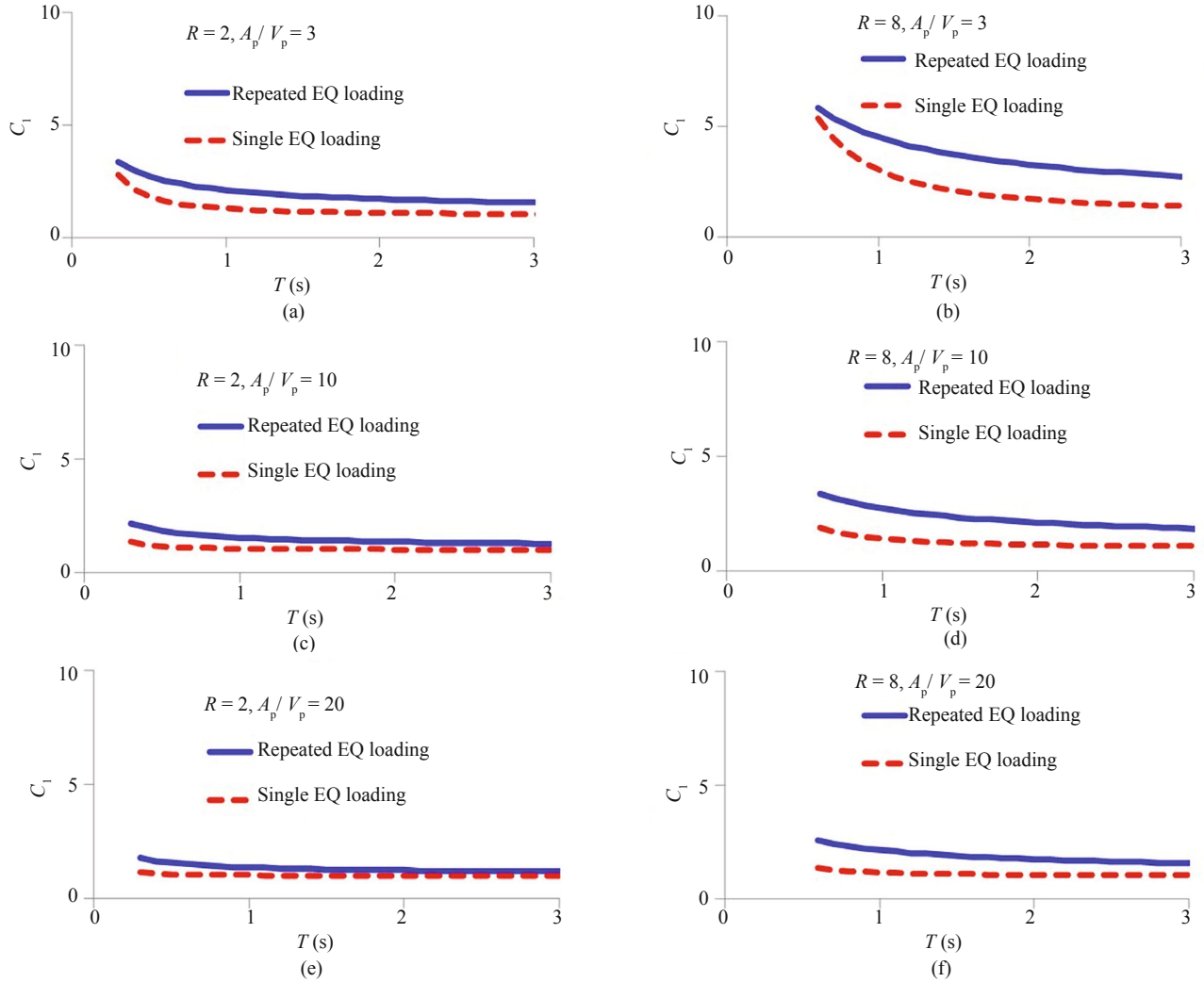

Fig. 7 C1 values for single earth quake loading vs. C1 values for repeated earthquake loading for; a) A_p/V_p = 3 and R = 2, b) A_p/V_p = 3 and R = 8, c) A_p/V_p = 10 and R = 2, d) A_p/V_p = 10 and R = 8, e) A_p/V_p = 20 and R = 2, f) A_p/V_p = 20 and R = 8

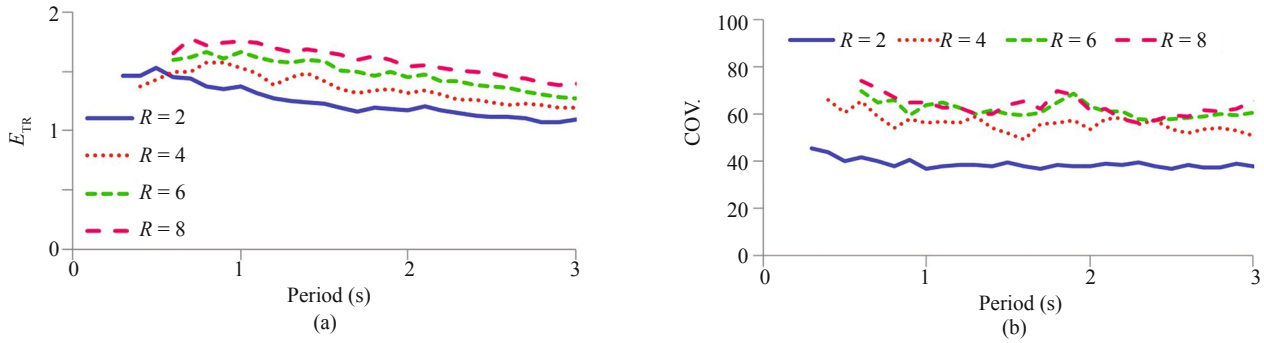

Fig. 8 (a) Average error and (b) COV (%) of the C_1 data calculated using Eq. (3)

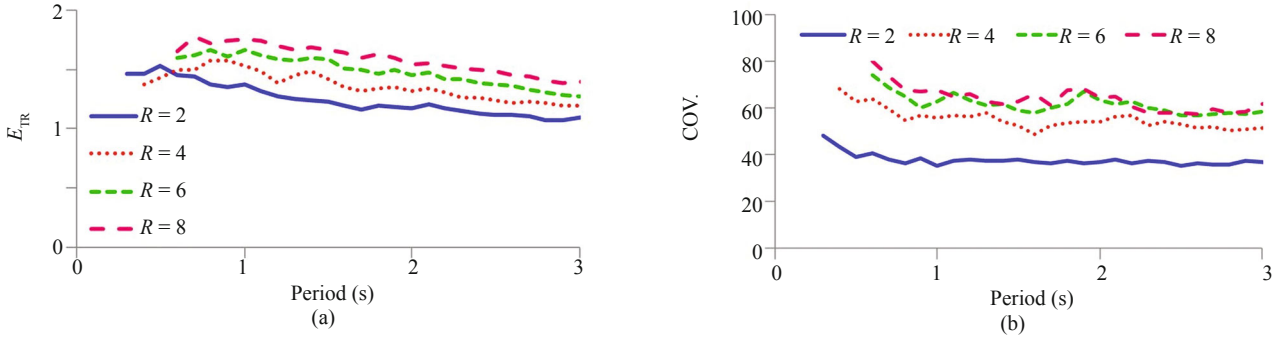

Fig. 9 (a) Average error and (b) COV (%) of the C_1 data calculated using Eq. (4)

R = 6 and 8), the deviation from 1 is more notable. Such a variation may be attributed to the unstable behavior and amplified record to record variability of relatively weak structures under repeated earthquake loading conditions. Furthermore, it is also observed that the level of deviation from Eq. (1) increases in the short period range. This also illustrates the amplified variability of C_1 values in the short period range. Similar comments are also valid for the plots showing the variation of COV values. From the Figs. 8(b) and 9(b) it is observed that for strong structures (i.e., R = 2), the ratio of standard deviations to the mean values are nearly constant for all period ranges. However for weaker structures, the value of COV increases for shorter period ranges. Another observation from the comparison of Figs. 8 and 9 is the fact that Eqs. (3) and (4) yield similar results in terms of presented error measurements.

In this study, a more convenient error measurement method is also applied to discover the more realistic error distribution of the proposed equations. In this method, the ground motion records with similar peak ground motion parameters (i.e., A_p/V_p for the error measurement of Eq. (3) and V_p for the error measurement of Eq. (4)) are grouped together. These groups consist of seven ground motion records due to the fact that average accelerograms of at least seven ground motion records may be used as a single ground motion loading in the time history analyses of structures (FEMA, 2000). Using the average value of accelerograms in the design and analyses procedures reduces the effect of exceptional acceleration values that may arise in the analyses. Similarly, the error measurements performed by using the averaged nonlinear time history analyses results provide more realistic and smooth results. In this regard, the mean analyses results obtained from these ground motion groups are treated as the result of a single ground motion record. Then, their mean peak ground motion parameter (i.e., A_p/V_p for the error measurement of Eq. (3) and V_p for the error measurement of Eq. (4)) value is used in the proposed equations to calculate the estimated C_1 value. The plots given in Figs. 8 and 9 are re-plotted in Figs. 10 and 11 for the error measurements of Eqs. (3) and (4), respectively. In the calculations, Eq. (5) is used by replacing the subscript "i" by subscript "G" to denote that the associated variable represent the mean value obtained from the analyses of a ground motion group. From the analyses results it is observed that mean error values are close to one but still stay on the safe side and may be used in the structural analyses.

In summary, from the statistical error estimations, it may be concluded that the accuracy of the proposed equations are acceptable. The proposed equations may be enhanced by introducing new parameters or using more complicated functional forms.

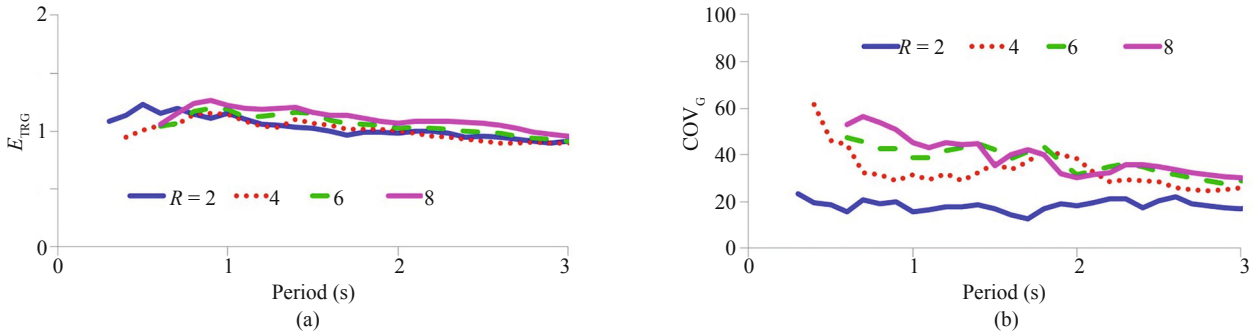

Fig. 10 (a) Average error and (b) COV (%) of the C_1 data calculated using Eq. (3) for grouped ground motions

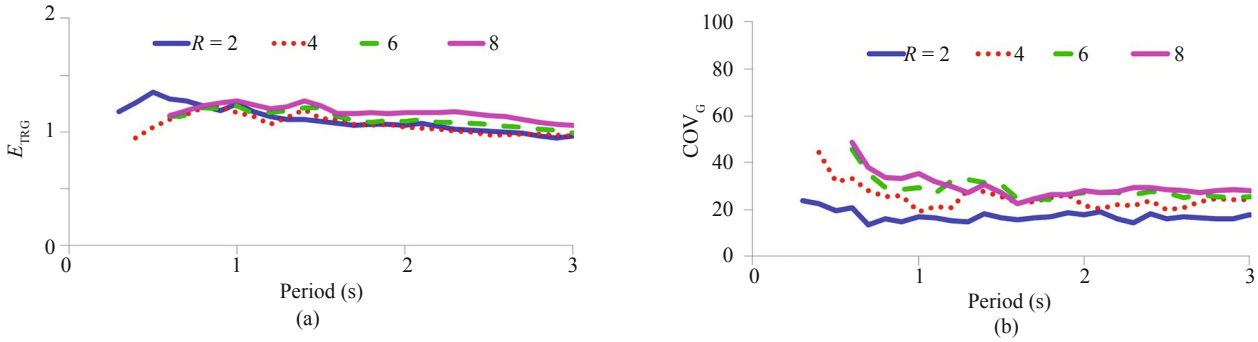

Fig. 11 (a)Average error and (b) COV (%) of the C_1 data calculated using Eq. (4) for grouped ground motions

10 Summary and conclusions

This study is aimed at developing statistical equations for the estimation of C_1 of SDOF systems subjected to FF repeated earthquake loading. In the proposed equations, the A_p/V_p ratio and V_p of the considered ground motion records are directly used. In the scope of the study, 306 ground motion records from 40 main shocks are used for the development and verification of the proposed equation. The main advantages of the proposed equations are: (i) simple functional form, (ii) large ground motion pool used in the derivation procedure, (iii) ground motion pool excludes the NF ground motion records with and without special pulse type characteristics, and (iv) direct use of peak ground motion parameters. To the authors' knowledge, this is the first study combining these specific properties for structures subjected to FF repeated ground motion records. Results of the study revealed that the C_1 values estimated by using the proposed equations are in good agreement with the results calculated by nonlinear dynamic time history analyses. Specific conclusions of the study are as follows:

- The C_1 values of ground motion records with smaller A_p/V_p ratios lead to higher C_1 ratios. In contrast, the C_1 values of ground motion records with higher V_p ratios lead to higher C_1 ratios.
- Direct use of A_p/V_p or V_p in the prediction of the C_1 ratio reduce record to record variability and yields accurate results by covering the bandwidth formed by the analyses results of repeated FF ground motion records.
- The equation proposed by ASCE-SEI (2007) yields results smaller than the actual results, especially for ground motions with high damaging potential.
- Results of the study revealed that the effect of repeated loading is considerable for SDOF systems subjected to repeated FF ground motion records. The effect of repeated loading is more pronounced for weaker structures and structures subjected to stronger ground motion loadings.
- The proposed statistical equations accurately estimate the C_1 of strong SDOF systems (i.e., $R \leq 4$). For weaker structures (i.e. $R \geq 6$), results calculated using the proposed equations stay on the conservative side, providing the capability to cover the uncertainties due to the weakness of structures.

References

Akkar S and Kucukdogan B (2008), "Direct Use of PGV for Estimating Peak Nonlinear Oscillator Displacements," *Earthquake Engineering &Structural Dynamics*, **37**(12): 1411–1433.

Akkar S and Bommer JJ (2005), "Empirical Prediction Equations for Peak Ground Velocity Derived from Strong-Motion Records from Europe and the Middle East," *Bulletin of the Seismological Society of America*,

97(2): 511–530.

Akkar S and Özen Ö (2005), "Effect of Peak Ground Velocity on Deformation Demands for SDOF Systems," *Earthquake Engineering & Structural Dynamics*, **34**(13): 1551–1571.

American Society of Civil Engineers (2007), *Seismic Rehabilitation of Existing Buildings*, ASCE/SEI Standard.

Applied Technology Council (2005), "Improvement of Nonlinear Static Seismic Analysis Procedures," *Report FEMA 440*, Federal Emergency Management Agency, Washington, DC, 2005.

Ay BÖ and Akkar S (2014), "Evaluation of a Recently Proposed Record Selection and Scaling Procedure for Low-Rise to Mid-Rise Reinforced Concrete Buildings and Its Use for Probabilistic Risk Assessment Studies," *Earthquake Engineering & Structural Dynamics*, **43**(6): 889–908.

Aydemir ME (2013), "Inelastic Displacement Ratios for Evaluation of Stiffness Degrading Structures with Soil Structure Interaction Built on Soft Soil Sites," *Structural Engineering and Mechanics*, **45**(6): 741–758.

Bates DM and Watts DG (1988), *Nonlinear Regression Analysis and Its Applications*, New York: Wiley.

Building Seismic Safety Council (2000), *Pre-Standard and Commentary for the Seismic Rehabilitation of Buildings*, FEMA-356, Federal Emergency Management Agency, Washington DC.

Changhai Z, Duofa J, Weiping W, Cuihua L, Weidong L and Lili X (2018), "Hysteretic Energy Prediction Method for Mainshock-Aftershock Sequences," *Earthquake Engineering and Engineering Vibration*, **17**(2): 277–291.

Chopra AK and Chintanapakdee C (2004), "Inelastic Deformation Ratios for Design and Evaluation of Structures: Single-Degree-of-Freedom Bilinear Systems," *Journal of Structural Engineering*, **130**(9): 1309–1319.

Cosenza E and Manfredi G (2000), "Damage Indices and Damage Measures," *Prog. Struct. Engng Mater*., **2**: 50–59.

Durucan C and Durucan AR (2016), "A_p/V_p Specific Inelastic Displacement Ratio for the Seismic Response Estimation of SDOF Structures Subjected to Sequential near Fault Pulse Type Ground Motion Records," *Soil Dynamics and Earthquake Engineering*, **89**: 163–170.

Durucan C and Dicleli M (2015), "A_p/V_p Specific Inelastic Displacement Ratio for Seismic Response Estimation of Structures," *Earthquake Engineering & Structural Dynamics*, **44**(7): 1075–1097.

Erduran E and Kunnath SK (2010), "Enhanced Displacement Coefficient Method for Degrading Multi-Degree-of-Freedom Systems," *Earthquake Spectra*, **26**(2): 311–326.

Faisal A, Majid TA and Hatzigeorgiou GD (2013), "Investigation of Story Ductility Demands of Inelastic Concrete Frames Subjected to Repeated Earthquakes," *Soil Dynamic and Earthquake Engineering*, **44**: 42–53.

Fajfar P and Fischinger M (1988), "N2—a Method for Nonlinear Seismic Analysis of Regular Structures," *Proc., 9th World Conferance on Earthquake Engineering*, **5**: 111–116.

Gutenberg B and Richter CF. (1944), "Frequency of Earthquakes in California," *Bull Seism Soc Am,* **34**: 185–188.

Hatzigeorgiou GD and Beskos DE (2009), "Inelastic Displacement Ratios for SDOF Structures Subjected to Repeated Earthquakes," *Engineering Structures*, **31**(11): 2744–2755.

Hatzigeorgiou GD (2010a), "Behavior Factors for Nonlinear Structures Subjected to Multiple Near-Fault Earthquakes," *Computers and Structures*, **88**: 309–321.

Hatzigeorgiou GD (2010b), "Ductility Demand Spectra for Multiple Near-And Far-Fault Earthquakes," *Soil Dynamics and Earthquake Engineerin*g, **30**: 170–183.

Iervolino I, Chioccarelli E and Baltzopoulos G (2012), "Inelastic Displacement Ratio of Near-Source Pulse-Like Ground Motions," *Earthquake Engineering and Structural Dynamics*, **41**(15): 2351–2357.

Joyner WB and Boore DM (1982), "Prediction of Earthquake Response Spectra," *USGS Openfile report*, 82–977.

Kabongo-Booto G, Hatzigeorgiou GD (2013), "Inelastic Displacement Ratio Spectrum for Near-Fault Ground Motions," *International Journal of Engineering and Technology*, **5**(6): 694–697.

Liu T and Zhang Q (2016), "A_p/V_p Specific Equivalent Viscous Damping Model for Base-Isolated Buildings Characterized by SDOF Systems," *Engineering Structures*, **111**: 36–47.

Miranda E (1999), "Approximate Seismic Lateral Deformation Demands in Multistory Buildings," *Journal of Structural Engineering*, *ASCE*, **125**(4): 417–425.

Miranda E (2001), "Estimation of Inelastic Deformation Demands of SDOF Systems," *Journal of Structural Engineering*," **127**(9): 1005–1012.

Miranda E (1991), "Seismic Evaluation and Upgrading of Existing Structures," *PhD Thesis*, University of California, Berkeley, Berkeley, Calif.

Muria Vila D and Toro Jaramillo AM (1998) "Effects of Several Events Recorded at a Building Founded on Soft Soil," *11th European Conference on Earthquake Engineering*, Paris.

Pacific Earthquake Engineering Research Center (PEER), Strong Ground Motion Database, http://peer.berkeley.edu/, [30.01.14].

Ruiz-García J and Miranda E (2003), "Inelastic Displacement Ratios for Evaluation of Existing

Structures," *Earthquake Engineering &Structural Dynamics*, **32**(8): 1237–1258.

Ruiz-García J and Miranda E (2006), "Inelastic Displacement Ratios for Evaluation of Structures Built on Soft Soil Sites," *Earthquake Engineering & Structural Dynamics*, **35**(6): 679–694.

Ruiz-Garcia J (2011), "Inelastic Displacement Ratios for Seismic Assessment of Structures Subjected to Forward-Directivity Near-Fault Ground Motions," *Journal of Earthquake Engineering*, **5**(3): 449-468.

Ruiz-Garcia J (2012), "Mainshock-Aftershock Ground Motion Features and Their Influence in Building's Seismic Response," *Journal of Earthquake Engineering*, **16**(5):719–737.

Shcherbakov R, Turcotte DL and Rundle JB (2005), "Aftershock Statistics," *Pure and Applied Geophysics*, **162**: 1051–1076.

Trombetti T, Silvestri S, Gasparini G, Righi M and Ceccoli C (2008), "Correlations Between the Displacement Response Spectra and the Parameters Characterizing the Magnitude of the Ground Motion," *14. World Conference on Earthquake Engineering*, Beijing, China.

Veletsos AS and Newmark N (1960), "Effect of Inelastic Behavior on the Response of Simple Systems to Earthquake Motions," *Proceedings of the 2nd World Conference on Earthquake Engineering*, **2**: 895–912.

Yaghmaei-Sabegh S (2012), "Application of Wavelet Transforms on Characterization of Inelastic Displacement Ratio Spectra for Pulse-Like Ground Motions," *Journal of Earthquake Engineering*, **16**(4): 561–578.

Zhai C, Wen W and Ji D (2015), "The Influences of Aftershocks on the Constant Damage Inelastic Displacement Ratio," *Soil Dynamics and Earthquake Engineering*, **79**: 186–189.